PNAS

Supplementary Information for
Biogeochemical fingerprinting of magnetotactic bacterial magnetite

Alberto Pérez-Huerta, Chiara Cappelli, Ylenia Jabalera, Tanya Prozorov, Concepción Jimenez-López,

Dennis A. Bazylinski

Alberto Perez-Huerta
Email: aphuerta@ua.edu

This PDF file includes:

Supplementary text
Figures S1 to S7
Tables S1 to S4
SI References

Supplementary Information Text

Samples

- *Bacterial magnetite (BM)*: Magnetite nanoparticles were obtained from magnetosomes precipitated by *Magnetospirillum gryphiswaldense* MSR-1 (1) (Fig. 1 in Main Text). To obtain these magnetite nanoparticles, isolation and purification of particles was carried out after the complete removal of the magnetosome membrane. Once the cells were disrupted, the magnetic fraction that contained the magnetosomes was purified by using the variable opening magnet method as described in Bazylinski *et al.* (2). Magnetosomes were washed 25 times in buffer (20 mM Tris-HCl pH 7.1). All the washes were performed by using a Pasteur pipette, while the tubing was always in contact with the magnet, with a time between every washing cycle of 12 minutes. After the last wash, magnetosomes were suspended in buffer 20 mM Tris-HCl containing 1 % SDS to eliminate the magnetosome membrane. The use of SDS is a common procedure to purify magnetite from the magnetosome membrane (3-5). This suspension was incubated for 3 hours at room temperature, with an occasional stirring. After that, the suspension was centrifuged at 14,000 rpm (2 min, 4 ºC) and the pellet was recovered, dried, and stored under N_2 in an Eppendorf tube until FIB specimen preparation.

- Magnetite nanoparticles: Two set of abiogenic samples, one with untreated particles (IM) and another washed with SDS (IM-SDS) (Fig. 1 in Main Text), were produced. The synthesis of these magnetite nanoparticles was carried out at 25 °C and 1 atm total pressure inside at anaerobic chamber filled with 4% H_2 in N_2 (6). Abiogenic magnetic nanoparticles were precipitated from this mixture reaction: 2.78 mM $Fe(ClO_4)_2$, 5.56 mM $FeCl_3$, at a pH value of 9. Biomimetic magnetic nanoparticles (BMNPs) were

precipitated using the same mixture with carbonate buffer (3.5 mM) and recombinant MamC protein (10 µg/mL), at a pH value of 9. Samples were incubated for 30 days and then the solids were magnetically concentrated and washed. The magnetoliposomes (L-MNPs) synthesis was performed following the thin film hydration protocol (7). Briefly, magnetic nanoparticles were used to hydrate and disperse the lipid film layer composed by egg phosphatidylcholine (PC) (Avanti Polar Lipids, 6 mg/mL).

Methods

Focused Ion Beam (FIB) Work:

During the fabrication of APT tip-shaped specimens by FIB-SEM, deposition of the protected Pt layer on the samples surface may induce carbon contamination since the deposited gas produced by the GIS (Gas Injection System) also contains detectable C as $C_9H_{16}Pt$. It is worth noting that, upon adhering to a specific preparatory protocol for series of samples microfabricated using the same instrument, such a potential source of contamination could be present for nanoporous materials. However, we want to emphasize that the C attributed to contamination during FIB Pt deposition has a uniform and peripheral 3D distribution (see Fig. 3 in the main text) and accounts for a small percentage of the specimen bulk composition.

The University of Alabama Sample Preparation:

Isolated, purified magnetite particles extracted from *Magnetospirillum gryphiswaldense* MSR-1 formed a cohesive, thin compacted layer ("crust") (see Fig. S1). This compacted layer was placed on top of a cured resin block, fixed on the sides with silver paint, and gently polished on a Micro-cloth with 0.3 µm alumina suspension. After polishing, the surface was cleaned three times with DI water. The polished sample were then secured to an aluminum stub using conductive silver liquid paint and sputter coated with 15 nm of Cu before FIB-SEM work (8).

A rectangle of Pt was deposited on the polished section of the Cu coated magnetite using a Ga^+ ion beam at 30 kV and 100 nA over a 1.5 x 20 µm region. A wedge of material below the Pt rectangle was then cut using the ion beam (30 kV, 1 nA) on the three sides. This wedge was welded to an *in situ* nano-manipulator (SmarAct) using FIB-deposited Pt before cutting the final edge free. 1-2 µm wide segments were cut from the wedge and sequentially affixed with Pt to the tops of Si posts of a microtip array coupon purchased from CAMECA Scientific Instruments, Inc. Each specimen tip was shaped and sharpened using annular milling patterns of increasingly smaller inner and outer diameters. Initially, the milling was performed at 30 kV to produce the specimen geometry necessary for APT. Final milling was performed at an accelerating voltage of 5 kV in order to reduce Ga^+ implantation and obtain a consistent tip-to-tip shape. The diameter at the top of the tips for biomagnetite samples varied between 40-50 nm, while the shank angle of the tips ranged from 27 to 42° (Fig. S1). For the bacterial magnetite sample, the wedge generated 8 tips but only 3 yielded significant data (> 4.5 million ion count) for further data analysis and comparison see Table S1.

DOE Ames Laboratory Sample Preparation:

Preparation of tips from abiogenic magnetite nanoparticles (IM and IM-SDS), biomimetic magnetite nanoparticles (BMNPs), and magnetoliposomes (L-MNPs): Abiogenic magnetite and BMNPs nanoparticles were provided as dried powders, whereas the magnetoliposomes were in a pre-cooled solution and kept at 4 ^{0}C until ready to use. All of these nanoparticles were prepared using a similar protocol as follows: A small amount of magnetite powder was dispersed in 20 µL of nanopure water (18.2 MΩ-cm, 25 °C) and concentrated with a small magnet. ~5 mm of In wire was flattened with a fragment of silicon wafer, and a magnet was placed underneath the Si/In substrate. ~3 µL of concentrated magnetite suspension were transferred using a micropipette, deposited on top a flattened In/Si surface residing on top of a magnet, the excess of liquid was gently wicked away with lens paper, and allowed to air dry for 15 -20 min. The fragments of silicon wafer were cleaned with ethanol absolute (Decon Labs, Inc., PA) and plasma cleaned with UV ozone ProCleaner™ (Bioforce Nanosciences, Ames, IA, USA) for 30 min before use, to ensure removal of residual carbon. Using a clean Si square, the magnetite crust was pressed again to compact the nanoparticles into the indium. The surface of the compacted "crust" was coated with Au metal using a SPI-MODULE™ sputter with a current of ~18 mA for 90 seconds, yielding approximately 40 nm-thick Au layer. Au-sputtered specimen was then affixed to a regular Al stub using silver paint and transferred into the Helios NanoLab G3 UC Dual Beam FIB Microscope for the specimen tip preparation.

Tip Preparation (Fig. S2): A rectangle of Pt was deposited over a visually flat section of the Au-sputtered magnetite surface, using a Ga^+ ion beam at 30 kV and 80 pA, typically over a 2 μm x 35 μm region, yielding ~1.3 μm-thick protective layer of Pt. A wedge was then cut using the ion beam at 30 kV and 9.3 nA on the three sides (so-called J-cut approach). The compacted crust wedge was lifted-out using an EasyLift micromanipulator and mounted onto silicon micro-tip coupons using Pt to fill-in the gaps in four sides. Sharpening of the tips was carried out at 52° using an annular pattern to create first a cylindrical post and then a sharp tip at lower kV as following: 1) Initial milling was performed at 30 kV and 0.23 nA with inner radius of 1.5 μm; 2) Milling performed at 5 kV and 68 pA with inner radius 1 μm; 3) Milling performed at 5 kV and 41 pA with inner radius 700 nm; 4) Milling performed at 5 kV and 15 pA with inner radius 500 nm; 5) Final milling performed at 5 kV and 15 pA with inner radius 300 nm. Resultant magnetite micro-tips have a diameter between ~ 50 – 70 nm and a shank angle of ~ 40-60°. Following this protocol, several tips of the laboratory-synthesized nanoparticles were produced as follows: 23 tips of abiogenic magnetite (IM), 19 tips of abiogenic magnetite washed with SDS (IM-SDS), 14 tips of biomimetic magnetite grown in the presence of the magnetosome protein MamC (BMNPs), and 21 tips of imagnetite with liposomes (L-MNPs). Despite these large number of tips, all of which were run in the LEAP, tips were fragile and tip fracture was a common occurrence. As a consequence, no more than 5 tips of each sample yielded significant data with uniform voltage curves; the best three samples, except only two for L-MNPs, were used for comparison with the bacterial magnetite (Tables S1, S2 and S4).

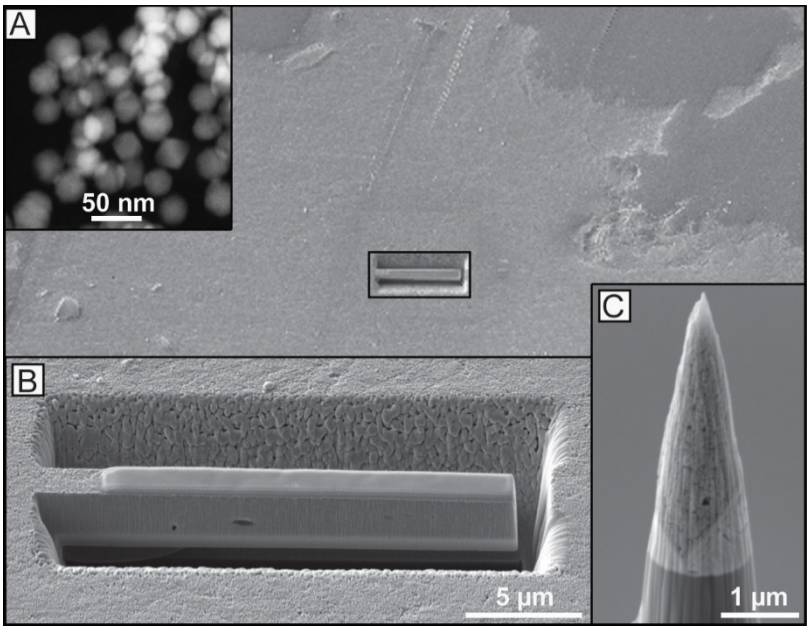

Figure S1. Scanning electron microscopy (SEM) image of the analyzed layer of tightly bound magnetite particles, after isolation and purification, from the magnetotactic bacterium *Magnetospirillum gryphiswaldense* MSR-1 (Note the black rectangle indicating location of the wedge extraction). (A) High angle annular dark field scanning transmission electron microscopy (HAADF-STEM) image to indicate the morphology and size of magnetosome magnetite nanocrystals. (B) Image of a wedge fabricated by focused ion beam on the thin layer of particles, showing the voids in between particles in a depth profile. (C) Example of an APT tip specimen composed of magnetite nanoparticles.

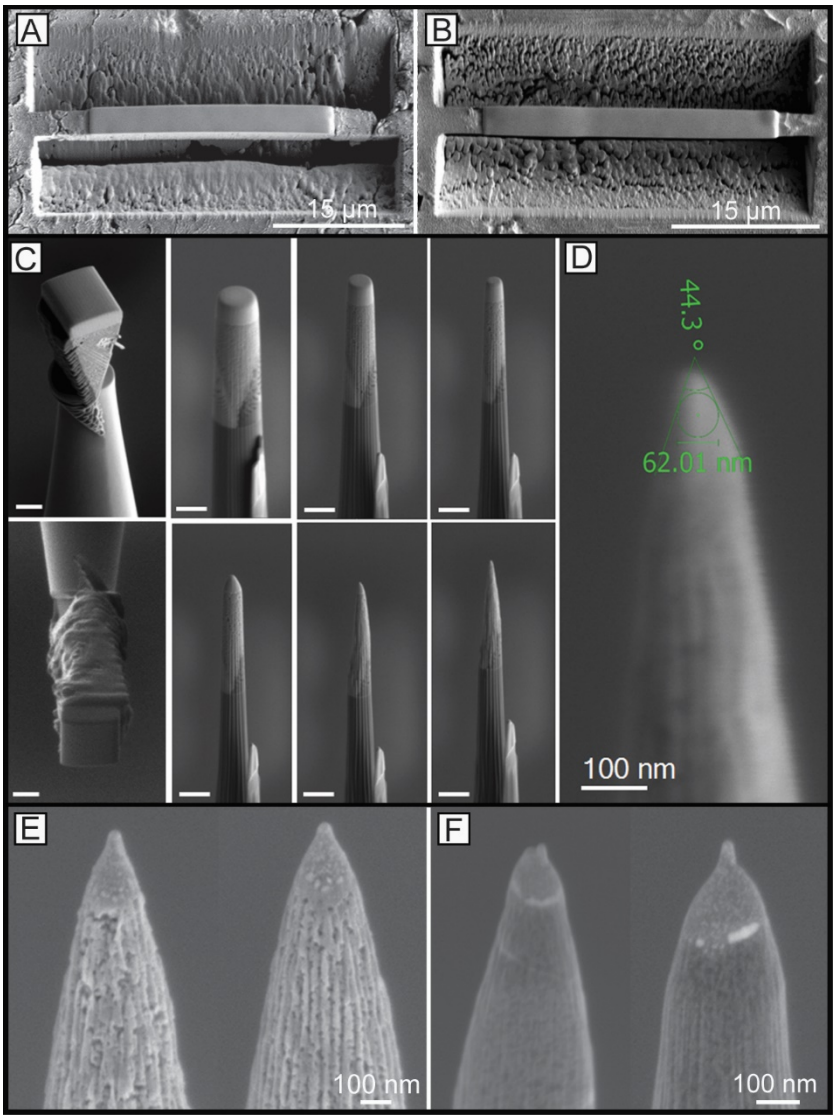

Figure S2. Sample images to illustrate the protocol of APT tip preparation for laboratory-synthesized nanoparticles. (A) Sample wedge in a crust of abiogenic particles (sample IM); (B) Sample wedge in a crust of biomimetic particles (sample BMNPs); (C) Sharpening procedure from a wedge fragment to a final tip shape (all scale bars = 1µm); (D) Example of a final tip shape, after low kV cleaning, with measurements of the tip radius and shank angle; (E) Examples of finals tips for sample IM; (F) Examples of final tips for sample BMNPs.

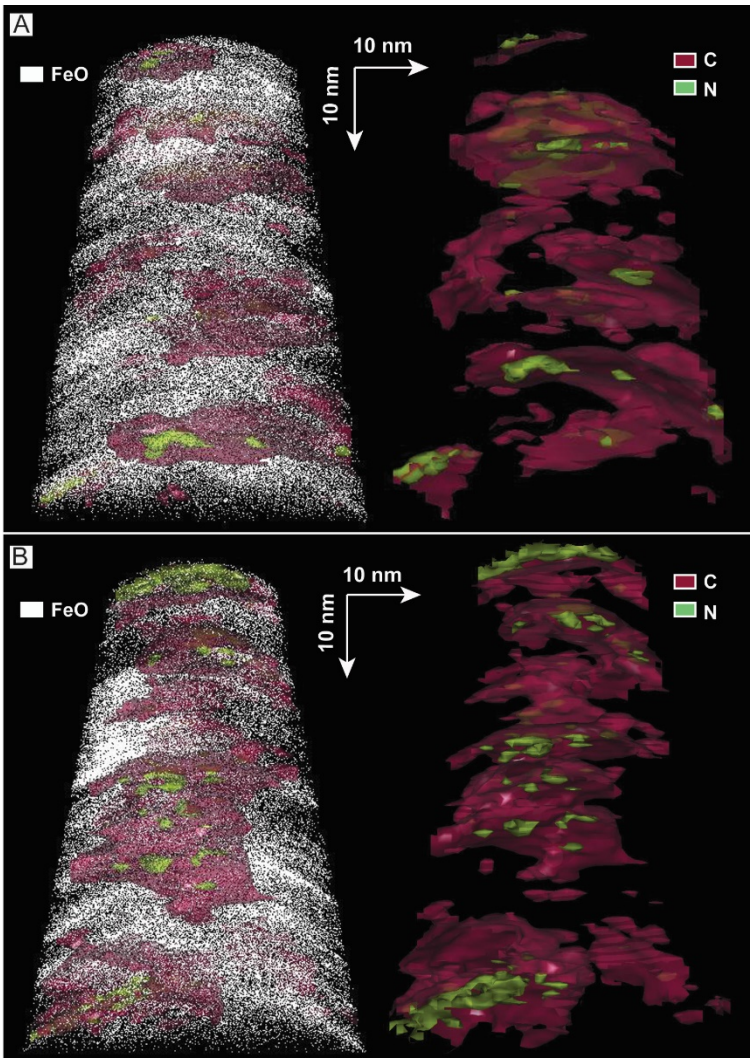

Figure S3. APT 3D reconstructions of bacterial magnetite tips 513 (A) and 571 (B) (Table S1). Note the presence of carbon and nitrogen (occupying spaces inside carbon layers), reconstructed as isosurfaces at the same atomic % as that measured for these elements in these tips (see Table S2), inside the magnetite (represented by the FeO atomic distribution).

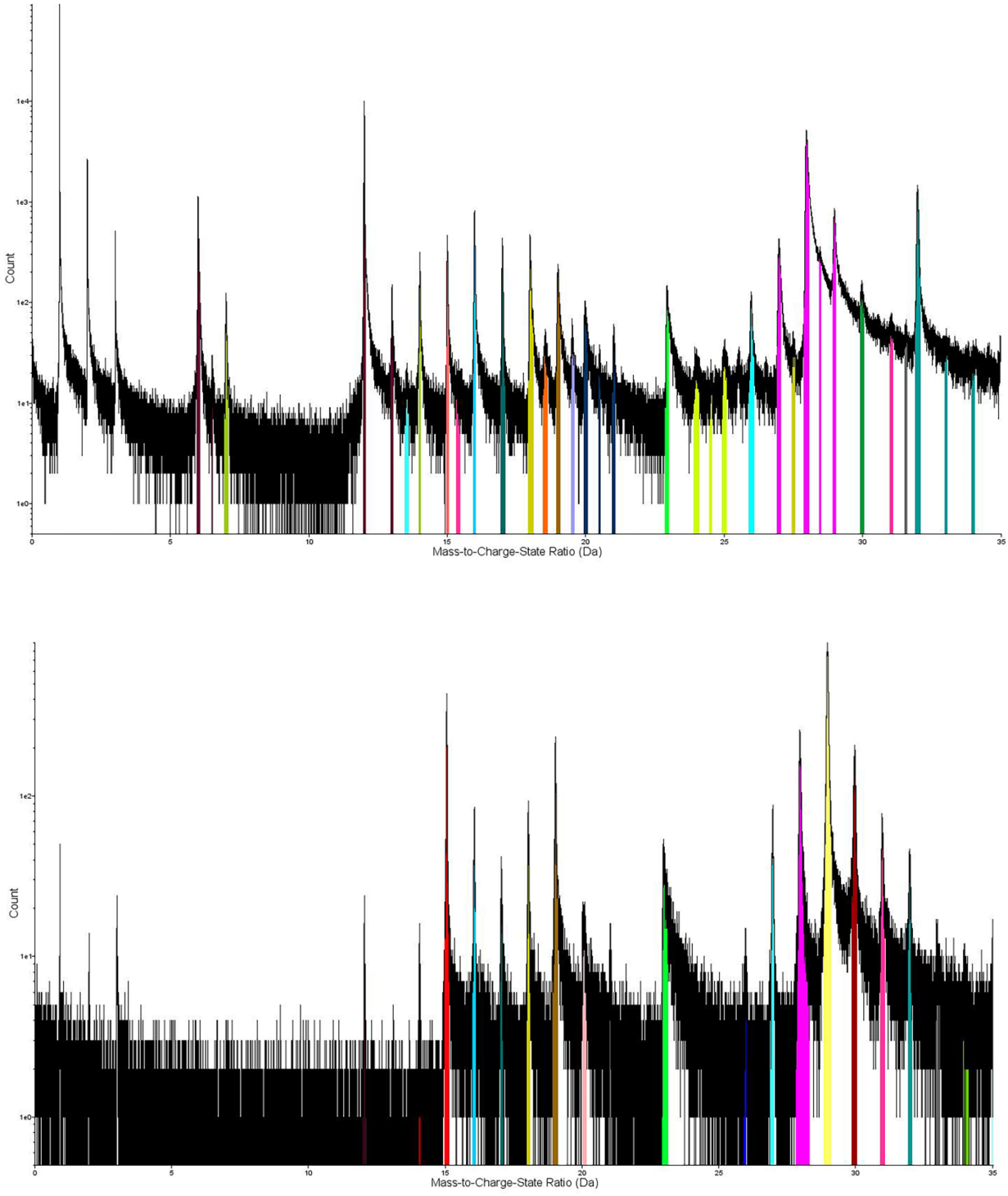

Figure S4. Comparison of the typical APT chemical spectra (up to 35Da) for bacterial magnetite (top; 513) and the abiogenic magnetite nanoparticle (sample IM) (bottom; 2775). Note that the bacterial magnetite spectrum is the only one containing C and N peaks at 2+ charge (6Da and 7Da); this is also the case for a comparison with spectra of the rest of laboratory-synthesized nanoparticles (see Fig. S5) [Note: Original IVAS files (RHIT and HITS) are available publicly at https://figshare.com/projects/Perez-Huerta_PNAS_Biomagnetite_APT_Files/143037].

A

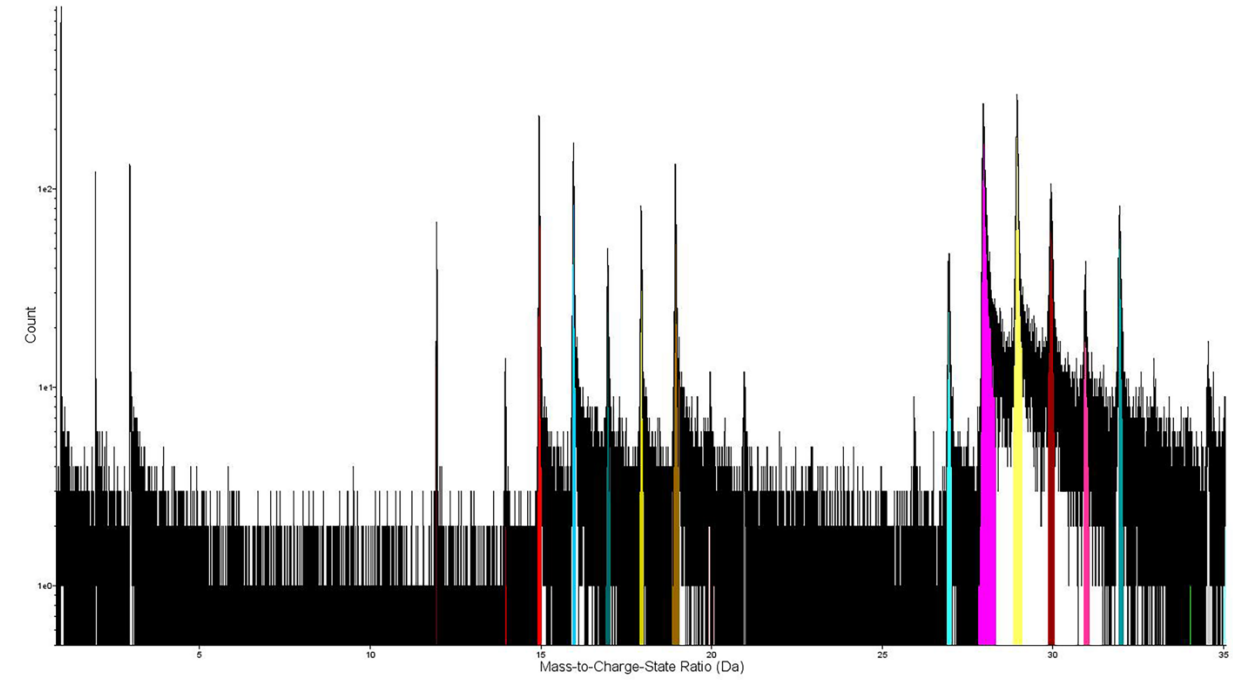
Count
1e2
1e1
1e0
5
10
15
20
25
30
35
Mass-to-Charge-State Ratio (Da)

B

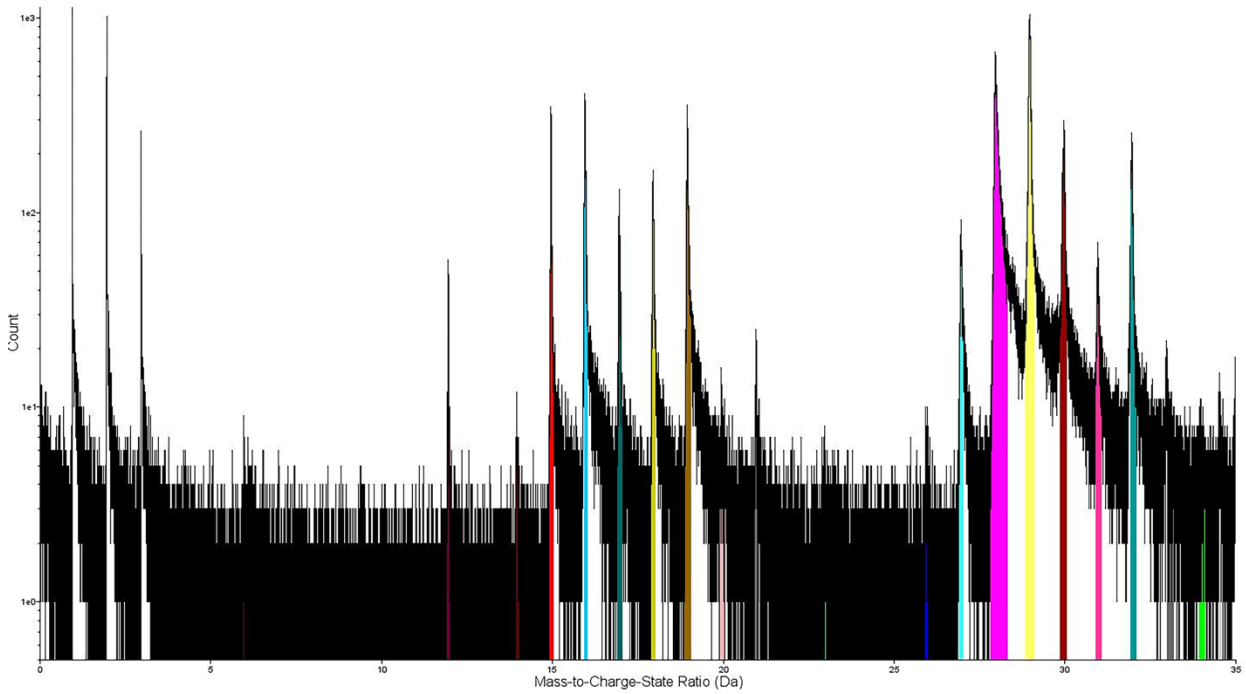
Count
1e3
1e2
1e1
1e0
0
5
10
15
20
25
30
35
Mass-to-Charge-State Ratio (Da)

C

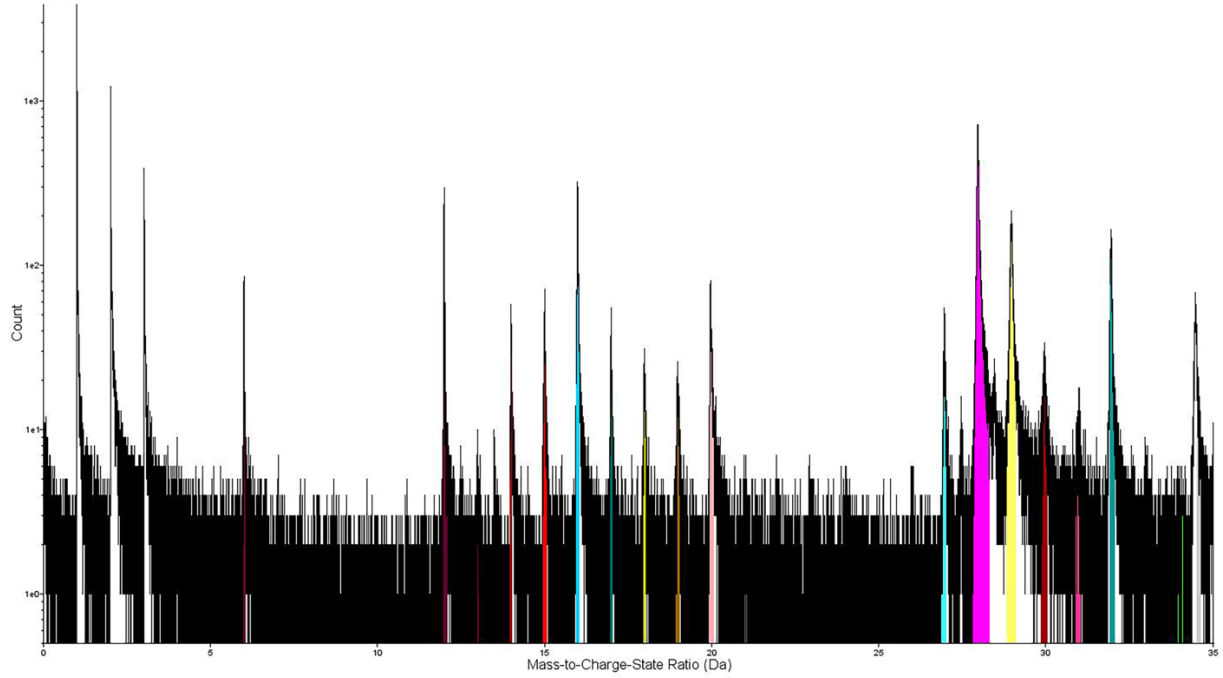

Figure S5. Comparison of the typical APT chemical spectra (up to 35Da) for abiogenic magnetite washed with SDS (IM-SDS; 3480) (**A**), biomimetic magnetite (BMNPs; 3468) (**B**), and magnetoliposomes (L-MNPs; 3733) (**C**). [Note: Note: Original IVAS files (RHIT and HITS) are available publicly at https://figshare.com/projects/Perez-Huerta_PNAS_Biomagnetite_APT_Files/143037].

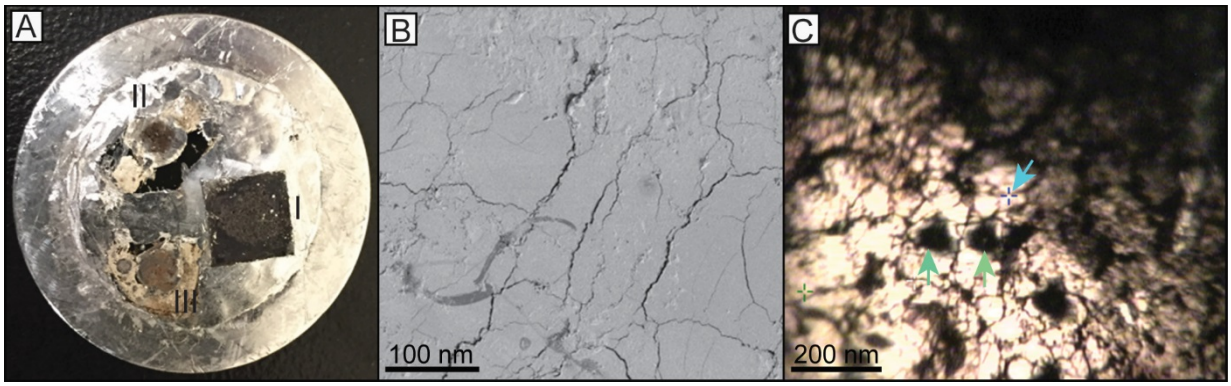

Figure S6. Example of sample preparation for SIMS analyses. (A) Polished samples [I – BM, II – BMNPs, and III – L-MNPs] in one-inch (2.54 cm) mount. (B) SEM image showing the surface of the multi-particle layer for sample L-MNPs. (C) Optical image of the surface of sample BM, showing the testing 30 μm spot size (green arrows) and the location of the 4 μm spot for analysis (blue arrow).

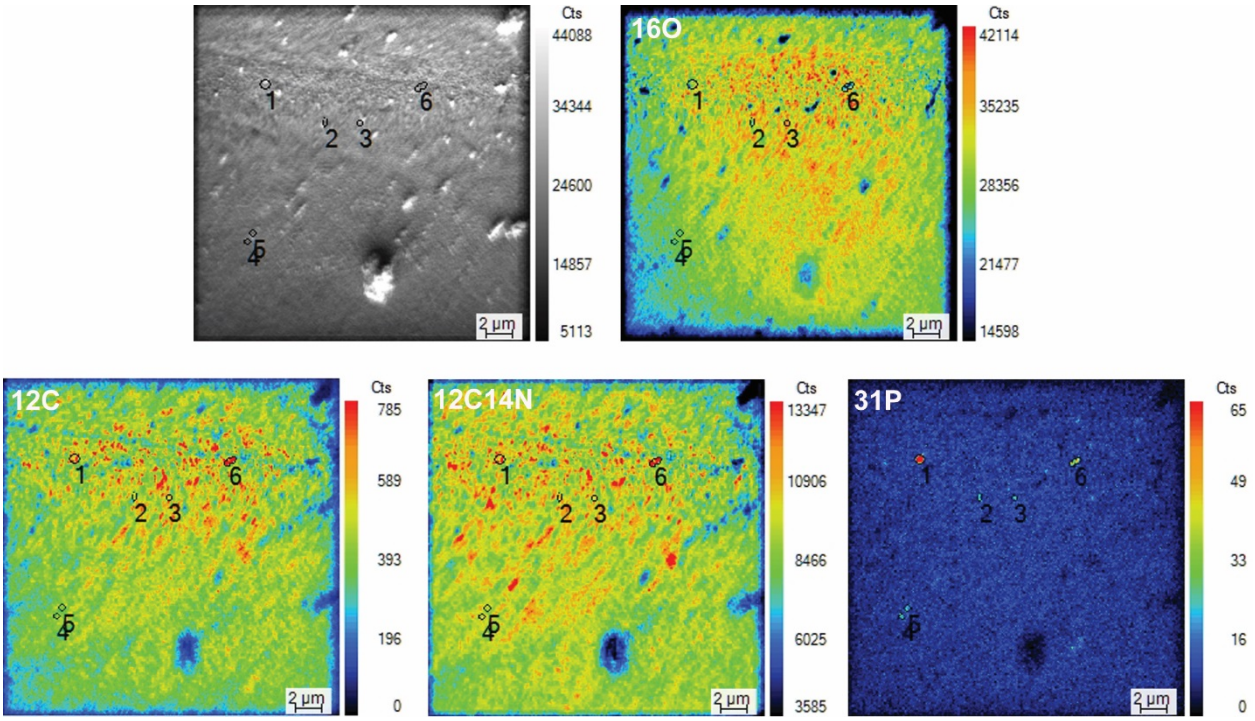

Figure S7. Nano-SIMS data for the bacterial magnetite multi-particle surface (see details in Materials and Methods in main text). Surface image (top left) and corresponding maps for the integrated counts of ^{16}O, ^{12}C, $^{12}C^{14}N$, and ^{31}P [Note – Numbers indicate locations of points to facilitate comparison among individual maps].

Table S1. Example of LEAP running conditions for biogenic magnetite (BM) tips and abiogenic magnetite nanoparticles (samples IM and IM-SDS) tips

Specimen/Data Set*	BM 513	BM 514	BM 571	IM 3705	IM 3702	IM 2775	IM-SDS 3479	IM-SDS 3476	IM-SDS 3480
Instrument Model	LEAP 5000 XR								
Instrument settings									
Laser wavelength (λ)	355								
Laser pulse energy (pJ)	30	30	30	30	30	30	30	30	30
Pulse frequency (kHz)	125	125	125	125	125	125	125	125	125
Evaporation control	Detection rate								
Target detection rate (ions/pulse)	0.2	0.2	0.2	0.2	0.2	0.2	0.2	0.2	0.2
Nominal flight path (mm)	100								
Set point temperature (K)	30	30	30	30	30	30	30	30	30
Sample temperature (K)	35	35	35	35	35	35	35	35	35
Chamber pressure (Torr)	8.00E-11	8.00E-11	8.20E-11	3.50E-11	3.60E-11	4.10E-11	4.90E-11	4.60E-11	5.30E-11
Data summary									
Analysis software	IVAS 3.8.4								
Total ions:	4769724	6165848	5801029	468766	394988	1423557	687426	557542	593920
Single (%)	80.2	65.6	73	80.1	83.2	82.8	88.4	84.7	81.2
Multiple (%)	18.4	33.1	25.7	17.8	13.6	14.3	6.3	12.4	15.9
Partial (%)	1.4	1.3	1.3	2.1	3.2	2.8	5.3	3	2.9
Reconstructed ions:	4500583	5808697	5380669	419970	338600	1360451	586402	486654	530249
Ranged (%)	42.6	43.2	45.7	55.0	41.4	48.5	51.1	41.4	46.0
Unranged (%)	57.4	56.8	54.3	45.0	58.6	51.5	48.9	58.6	54.0
Mass calib. (peaks/interp.)	Lin. Method								
(M/ΔM) for $_{28}Fe^{++}/_{44}FeO^{++}/_{29}SiH^{+}$	409	424	429	445	507	431	620	428	563
$(M/\Delta M_{10})^{c}$	103	115	117	127	172	163	251	172	226
Time independent background (ppm/ns)	33	32	36	29	41	37	39	47	35
Reconstruction									
Final specimen state	fractured	fractured	fractured	fractured	fractured	fractured	fractured	fractured	fractured
Pre-/post-analysis imaging	SEM/SEM								
Radius evolution model	Shank	Shank	Shank	Shank	Shank	Shank	Shank	Shank	Shank
Field factor (k)	3.3	3.3	3.3						3.3
Image compression factor	1.65	1.65	1.65						0.5
Assumed E-field (V/nm)	18	18	18	18	18	18	18	18	18
Detector efficiency (%)	80	80	80	80	80	80	80	80	80
Avg. atomic volume (nm^3)	0.0118	0.0118	0.0118	0.0118	0.0118	0.0118	0.0118	0.0118	0.0118
$V_{initial}$; V_{final} (kV)	1.3;4.1	1.0;4.0	1.2;4.6	1.7;3.0	1.2;2.7	1.3;2.4	1.3;3.8	1.2;2.5	1.2;2.7

*BM=Bacteria magnetite; IM=inorganic magnetite; IM-SDS=inorganic magnetite washed SDS

Table S2. Comparison of atom probe tomography (APT) concentrations (atomic %) for singly and doubly charged ion peaks at 6Da, 12Da, 7Da, 14Da, and 15Da (see Figure 2 in main text) in three analyzed tips of bacterial magnetite (BM) and abiogenic magnetite samples (IM and IM-SDS).

	Run	Peak	Ion	Counts	%	error	Peak	Ion	Counts	%	error	Peak	Ion	Counts	%	error
BM	513	6-12	C^+,C^{++}	316819	11.6	2.78E-04	7-14	N^+,N^{++}	14390	0.53	6.17E-05	15	NH^+	33277	1.22	6.75E-05
	514			443654	12.7	2.60E-04			21519	0.62	5.87E-05			31822	0.91	5.13E-05
	571			318055	8.5	2.01E-04			15144	0.40	4.56E-05			26011	0.69	4.31E-05
IM	3705	12	C^+	146	0.03	2.84E-05	14	Si^{++}/N^+	135	0.03	2.73E-05	15	BH_4^+/NH^+	22050	5.18	3.58E-04
	3702			-	-	-			50	0.02	2.50E-05			14410	5.09	4.35E-04
	2775			537	0.05	2.33E-05			374	0.04	1.95E-05			82845	8.33	3.01E-04
IM SDS	3479	12	C^+	1809	0.28	6.63E-05	14	Si^{++}/N^+	241	0.04	2.42E-05	15	BH_4^+/NH^+	34129	5.31	2.95E-04
	3476			209	0.05	3.59E-05			250	0.06	3.93E-05			61242	15.21	6.60E-04
	3480			1277	0.28	7.91E-05			287	0.06	3.75E-05			41056	9.07	4.68E-04

Table S3. Comparison of SIMS data (based on 3 individual analyses per sample; averages and corresponding standard mean error in bold) for all samples also analyzed with APT.

Specimen	BM		IM		IM-SDS		BMNPs		L-MNPs	
	$^{12}C/^{56}Fe$	$^{12}C/^{12}C^{14}N$	$^{12}C/^{56}Fe$	$^{12}C/^{12}C^{14}N$	$^{12}C/^{56}Fe$	$^{12}C/^{12}C^{14}N$	$^{12}C/^{56}Fe$	$^{12}C/^{12}C^{14}N$	$^{12}C/^{56}Fe$	$^{12}C/^{12}C^{14}N$
Analysis 1	533 (±2.37)	1.12 (±1.08)	7 (±1.22)	4.16 (±1.08)	7.39 (±2.13)	1.39 (±2.38)	285 (±4.40)	3.92 (±1.67)	1.63 (±1.68)	0.46 (±0.89)
Analysis 2	596 (±1.47)	1.98 (±0.4)	3.15 (±2.07)	0.96 (±2.70)	7.25 (±2.37)	0.88 (±1.34)	229 (±1.60)	5.17 (±4.79)	1.30 (±1.75)	0.43 (±0.74)
Analysis 3	1280 (± 4.41)	2.03 (±1.09)	3.44 (±2.23)	0.64 (±2.05)	4.28 (±2.19)	1.14 (±1.23)	414 (±3.37)	5.23 (±1.24)	1.13 (±2.34)	0.48 (±1.32)
Average	**803 (±1.34)**	**1.71 (±2.08)**	**4.53 (±1.31)**	**1.92 (±1.12)**	**6.3 (±1.17)**	**1.13 (±1.4)**	**309.3 (±1.06)**	**4.79 (±1.3)**	**1.35 (±1.25)**	**0.45 (±1.81)**

Table S4. Comparison of carbon measurements (for C+ at 12Da peak; see Figs. S5 and S6), of 3 tips (except for the magnetoliposomes (L-MNPS)) for laboratory-synthesized magnetite nanoparticles. Note that these values would correspond to contamination and are very different to those measured for bacteria magnetite (see Table 1 in main text).

	Specimen	Atom count	Atomic %	Total hit count
Magnetite (IM)	3705	146	0.03	468769
	3702	-		395024
	2775	537	0.05	1424766
Magnetite (IM-SDS)	3479	1809	0.28	687598
	3476	209	0.05	557861
	3480	1277	0.28	594146
Magnetite (BMNPs)	3468	1431	0.12	1526084
	2816	12817	1.28	1839294
	2781	451	0.11	768766
Magnetite (L-MNPS)	3733	9702	3.06	560187
	3734	7001	3.24	390572

SI References

1. T. Prozorov, *et al.*, Manganese incorporation into the magnetosome magnetite: magnetic signature of doping. *Eur. J. Mineral.* **26**, 457–471 (2014).
2. D. A. Bazylinski, A. J. Garratt-Reed, R. B. Frankel, Electron microscopic studies of magnetosomes in magnetotactic bacteria. *Microsc. Res. Tech.* **27**, 389–401 (1994).
3. E. Alphandéry, S. Faure, L. Raison, E. Duquet, P.A. Howse, D.A. Bazylinski, Heat production by bacterial magnetosomes exposed to an oscillating magnetic field*. J. Phys. Chem. C* **115**, 18-22 (2011).
4. M. Amor, V. Busigny, M. Durand-Dubief, F. Guyot, Chemical signature of magnetotactic bacteria. *Proc. Natl. Acad. Sci. U.S.A.* **112**, 1699-1703.
5. A. Basir, J. Wang, F. Guo, W. Niu, W. Jiang, Improved methods for mass production of magnetosomes and applications: a review. *Microbial Cell Factories* **19**, 197 (2020).
6. C. Valverde-Tercedor, *et al.*, Size control of *in vitro* synthesized magnetite crystals by the MamC protein of *Magnetococcus marinus* strain MC-1. *Appl. Microbiol. Biotechnol.* **99**, 5109–5121 (2015).
7. Y. Jabalera, A. Fernández-Vivas, G. R. Iglesias, Á. V. Delgado, C. Jimenez-Lopez, Magnetoliposomes of mixed biomimetic and inorganic magnetic nanoparticles as enhanced hyperthermia agents. *Colloids Surfaces B Biointerfaces* **183**, 110435 (2019).
8. K. Genareau, A. Perez-Huerta, F. Laiginhas, Atom probe tomography analysis of exsolved mineral phases. *J. Vis. Exp.* **2019** (2019).